PERGAMON

International Journal of Heat and Mass Transfer 45 (2002) 2191–2205

International Journal of HEAT and MASS TRANSFER

www.elsevier.com/locate/ijhmt

Combined free and forced convection in a corner

A. Ridha *

Laboratoire de Modélisation en Mécanique, CNRS: UMR 7607, Université Paris 6, Tour 66 – Case 162, 4 place Jussieu, 75252 Paris Cedex 05, France

Received 20 November 2000

Abstract

A formulation of the three-dimensional combined free and forced convection boundary-layer flow in a corner is derived and discussed in terms of the corner orientation with respect to the buoyancy force. The corner is imagined to be formed by the abutment of two quarter-infinite wedges along a side edge parallel to an incoming uniform stream. Based on this formulation, similarity-type solutions are derived for different boundary-layer regions corresponding to almost planar horizontal corners, the numerical solutions of which are found to be characterized by their non-uniqueness in the corner-layer with a secondary flow exhibiting varying and sometimes complex flow patterns in function of the flow parameters; the most interesting feature is perhaps the existence of two streamwise symmetrically disposed vortices arising in layers immediately adjacent to the corner-layer. © 2002 Elsevier Science Ltd. All rights reserved.

1. Introduction

Three-dimensional flow along streamwise corners, specifically in the absence of heat transfer, has attracted considerable attention for many decades now. The corner is usually supposedly formed by the intersection of two semi-infinite flat plates (at zero incident) with coplanar leading edges; this configuration provides a realistic model to some engineering applications such as flow near sharp edges, flow in rectangular ducts or in the vicinity of an airplane wing-body junction. Rubin and collaborators [1–3] have treated laminar flow along a concave rectangular corner with zero streamwise pressure gradient, and the same but with arbitrary corner angle has also been studied by Desai and Mangler [4], Barclay and Ridha [5] and Wilkinson and Zamir [6]. These works have shown that corner flow formulation is characterized by difficulties mainly related to derivation of boundary conditions for the corner layer, and in their numerical application namely due to their inherent algebraic decay nature [2]. Specifically, the former aspect turns out to be extremely delicate since similarity-type solutions for zero and non-zero streamwise pressure gradient alike are non-unique [7–9], for example the corner layer far-field boundary conditions give rise to a second solution besides the Blasius one for zero pressure gradient. Ridha [8] has considered the stability of the numerical solutions for such a situation and found that the Blasius solution is less stable than the newly found one. More recently, Dhanak and Duck [9] have examined the flow stability of the corner layer and a close examination of their results shows that those corresponding to the new solution compare favourably well with the experimental results of El-Gamal [10] and Zamir [11] for a rectangular corner laminar boundary layer flow.

In the above cited works, heat transfer effects have not been dealt with since their considerations add further difficulties to an already complicated problem. It is therefore not surprising to find that attention has been mainly focused first on forced convection situations where exact solutions can be derived when suction is applied at the corner walls [12], or on similarity solutions for the temperature field only [13]. In this spirit, combined laminar forced and free convection in a vertical corner in the presence of suction has been considered by the present author [14] where exact asymptotic suction profile-type solutions are obtained. Recently,

* Present address: Laboratoire de Mécanique, Modélisation Mathématique et Numérique, Université de Caen, BP 5186, 14032 Caen Cedex, France.

E-mail address: ridha@meca.unicaen.fr (A. Ridha).

0017-9310/02/$ - see front matter © 2002 Elsevier Science Ltd. All rights reserved.
PII: S0017-9310(01)00302-7

Nomenclature

$\mathscr{A}, \mathscr{B}$	thermal effects terms in the corner layer, cf. Eqs. (4.15), (4.16) and (4.20)
c	an arbitrary parameter, $\sqrt{2/1+m}$
f_x, f_y, f_z	ratios of buoyancy to inertia forces in the x-, y- and z-directions
g	crossflow similarity solution, cf. Eq. (3.10)
g^*	gravitational acceleration
h	similarity stream function, cf. Eq. (3.9)
F, H, G	corner layer similarity solutions
Gr	Grashof number, $\beta^* g^* l^3 \triangle T/\nu^2$
J	dimensionless Jacobian of coordinates transformation, $n^2\rho^{2(n-1)}$
K	corner angle parameter, $\alpha \ln Re$
l, U_∞	characteristic length and velocity scales
m	exponent in the power law variation of the flow variables
M	a constant greater than 2
n	a parameter, $(\pi - 2\alpha)/\pi$
p	fluid pressure
q	an arbitrary parameter
r	dimensional/dimensionless radial coordinate
r_0	radial distance defining region I, $\delta l(z/l)^{(1-m)/2}$
Re	characteristic Reynolds number, $U_\infty l/\nu$
s	a parameter, $2\pi/(\pi - 2\alpha)$
T	dimensional/dimensionless fluid temperature
ΔT	temperature difference scale
u, v, w	dimensional/dimensionless velocity components in the x-, y-, z-directions
U, V, W	inviscid flow velocity components in the x-, y-, z-directions
$\mathscr{U}$	$(1 - 4K\alpha/\pi^2)\exp(-2K/\pi)$
x, y, z	dimensional/dimensionless Cartesian coordinates
z_g	a vertical ascendant Cartesian coordinate
Z	$\kappa\delta U_\infty (z/l)^{(m-1)/2}$, $c^{-1} z^{(m-1)/2}$

Greek symbols

α	defines corner angle by $\pi - 2\alpha$
α_w	wedge opening angle
β	an arbitrary parameter, $2m/m+1$
β^*	coefficient of thermal expansion
δ	a gauge parameter defining potential flow region I, $\delta \sim r/z$
δ^*	corner layer thickness, cf. Fig. 2
(δ_x, δ_y)	boundary layer (width,thickness) in the x-, y-directions
$(\varepsilon_x, \varepsilon_y)$	boundary layer velocity gauge parameters in the $x-$, y-directions
ξ, η, ζ	similarity solution independent variables
θ	temperature similarity solution
μ	a parameter, $(1-m)/2n$
ϑ	angular co-ordinate in the cylindrical polar co-ordinates system (z, r, ϑ), cf. Eq. (4.8)
ν	kinematic viscosity
ρ	radial coordinate in the polar system (ρ, χ), cf. Eq. (4.8)
ρ_∞	free-stream fluid density
σ	buoyancy parameter
κ^*	fluid thermal diffusivity
χ	angular coordinate in the polarsystem (ρ, χ), an implicit function of $(\mathscr{G}, \theta)$
ψ	a stream function, cf. Eq. (3.9)
γ	a short hand for $(2\xi - 1)/(\ln \xi - 1)$
ω	modified streamwise vorticity definition, cf. Eq. (4.14)

Subscripts

$0, 1, 2, \cdots$	variable in a series expansion
∞	free-stream value of a fluid property

laminar natural convection in a vertical corner has been examined [15] and similarity-type solutions are again found to be non-unique for this situation in the same sense as those reported in [7–9] for streamwise flow in corners with non-zero pressure gradient. To the author's knowledge, no work (apart from [14]) has been reported in the literature on mixed convection in a corner, reasons behind such an absence stemming mainly from difficulties presented by the potential flow problem corresponding to the corner flow geometry, since to study mixed convection in corners and derive similarity solutions requires a knowledge of the potential flow along corners formed essentially by intersecting wedges, see Fig. 1. This latter problem has been considered recently by the present author [16,17] who has shown that the inviscid flow can be divided into four distinct regions for which asymptotic representations have been derived. (See Fig. 2). This potential flow property leads to dividing the viscous motion into five distinct boundary layer regions as depicted on the same figure. Accordingly, two symmetrically disposed closed streamwise vortices are found in the intermediate layers [17], specifically in regions (iii) as illustrated in Fig. 1, thereby confirming a prediction made by Moore [18] that remained, until then, unconfirmed in the literature.

In this paper we investigate mixed convection exclusively (but without significant loss of generality) in almost planar corners and study in particular its effect on

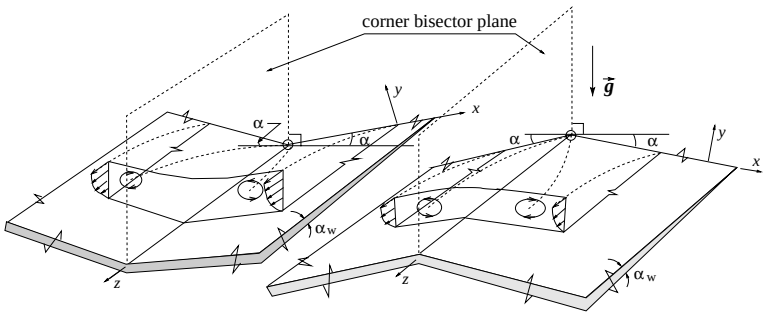

Fig. 1. Corner flow configuration: (x, y, z) is a Cartesian coordinates system the origin of which is placed at the corner vertex, the axes z coinciding with the corner line while $y = 0$ defining one of the corner surfaces. The corner bisector plane makes an angle of $(\pi - 2\alpha)/2$ with each of the corner walls which implies $\alpha > 0$ for concave corners and $\alpha < 0$ for convex ones.

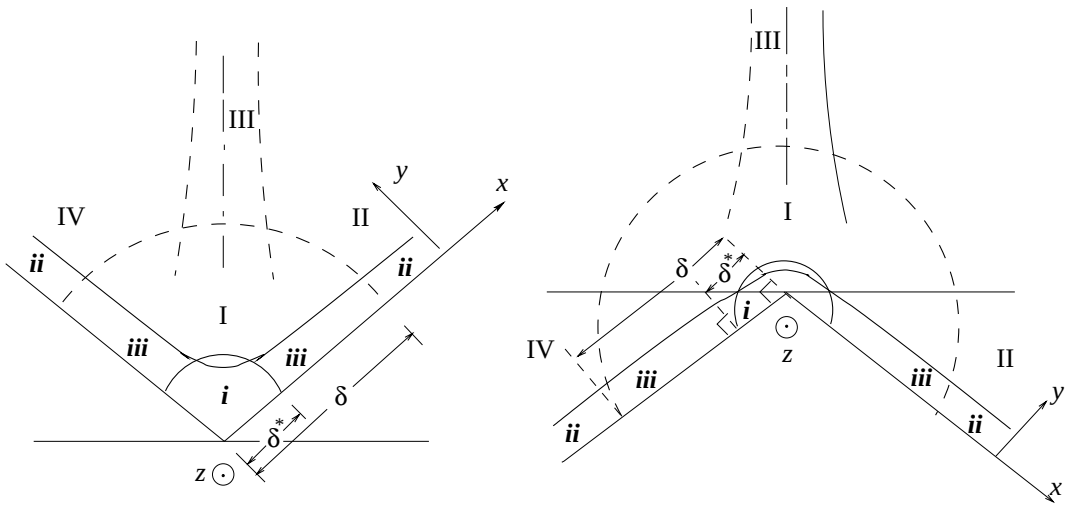

Fig. 2. A cross-section of the corner showing the potential (in broken lines) and viscous (in solid lines) flow regions in the corner vicinity: region I is characterized by $Re^{-1/2} \ll (r/z) \sim \delta \ll 1$, II and IV correspond to two-dimensional flows past a wedge with three-dimensional effects arising from their mutual interaction through regions I and III, the latter being a narrow cushion-like zone which absorbs the incompatibility of II and IV, see [16,17]. The viscous regions (i), (iii) and (ii) are three-dimensional boundary-layer zones; in (i) $(x, y) \sim \delta^*$, in (iii) $x \sim \delta$, $y \sim Re^{-1/2}$ and in (ii) $x \gg \delta$, $y \sim Re^{-1/2}$, δ^* being the corner-layer thickness. The z-axis is drawn pointing perpendicularly out of the page. For more details see [17].

the streamwise vorticity in the intermediate layers, regions (iii). First, after giving a brief description in Section 2 of the potential flow and its consequences on the boundary layer motion, the mixed convection problem in a corner is posed and a general formulation thereof is derived. In Section 3 mixed convection boundary layer equations are derived for the intermediate layers, region (iii); different possibilities are discussed according to the orientation of the corner walls and the corner line followed by deriving similarity-type solutions for almost horizontal corner walls as a case study. The corner layer problem is then considered in Section 4 where a general formulation of similarity-type solutions is derived followed by its application to almost planar horizontal corners. Some asymptotic features of the resulting equations are considered, and limits pertaining to concave or convex corners are derived and discussed.

Throughout, in order to avoid a heavy notation we have often reverted to mappings to retain the same symbols, the original definition can be recovered by following an inverse re-mapping sequence.

2. Formulation

To study combined free and forced thermal convection effect on viscous laminar steady flow along a streamwise corner of angle $\pi - 2\alpha$, we find it convenient

to consider corners formed by the abutment of two similar wedges (with coplanar leading edges) along a side edge as shown in Fig. 1, both wedges are assumed to have the same opening angle ($\alpha_w = \beta\pi$). Moreover, we assume that the corner is so oriented relatively to an incoming uniform stream (parallel to the corner line) that symmetry of the potential flow is assured with respect to the corner bisector plane. Here $\beta = 2m/(m+1)$ with m being an arbitrary constant. The potential flow problem (without thermal convection) has been studied in [16,17] where it is shown that a four-region treatment arises naturally for the inviscid flow as depicted in Fig. 2. Sufficiently near the corner walls, the inviscid flow velocity vector (U, V, W) associated with the Cartesian coordinates (x, y, z) assumes the following form [17]

$$U = Z\left[-\frac{1}{2}m\left(\frac{x}{r_0}\right) + \frac{m}{2(s-1)}\left(\frac{r}{r_0}\right)^{s-1}\cos(s-1)\vartheta\right] + \mathrm{O}(\delta^3), \tag{2.1}$$

$$V = Z\left[-\frac{1}{2}m\left(\frac{y}{r_0}\right) - \frac{m}{2(s-1)}\left(\frac{r}{r_0}\right)^{s-1}\sin(s-1)\vartheta\right] + \mathrm{O}(\delta^3), \tag{2.2}$$

$$W = U_\infty\left(\frac{z}{l}\right)^m + \mathrm{O}(\delta^2), \tag{2.3}$$

in region I, with $z > 0$. Here $Z = \delta U_\infty (z/l)^{(m-1)/2}$ and (r, ϑ, z) are cylindrical polar coordinates with $(x, y) = r(\cos\vartheta, \sin\vartheta)$. The corner walls are given by $\vartheta = 0$ and $\pi - 2\alpha$. At the inner limit of region II, the velocity vector is found to take the following form

$$U = \delta U_\infty \frac{m(2-s)}{2(s-1)}\left(\frac{z}{l}\right)^{(m-1)/2} + \mathrm{O}(\delta^3), \tag{2.4}$$

$$V = -U_\infty\left(\frac{y}{l}\right)\left(\frac{z}{l}\right)^{m-1} + \mathrm{O}(\delta^3), \tag{2.5}$$

$$W = U_\infty\left(\frac{z}{l}\right)^m + \mathrm{O}(\delta^2). \tag{2.6}$$

In Eqs. (2.1)–(2.6), we have $Re^{-1/2} \ll \delta \sim r/z \ll 1$, $r_0 = \delta l (z/l)^{(1-m)/2}$, $s = 2\pi/(\pi - 2\alpha)$; r_0 is related to the size of region I while l and U_∞ are length and velocity scales. The Reynolds number is given by $Re = lU_\infty/\nu$ in which ν designates the kinematic viscosity. Note that these equations are obtained by matching the respective velocity components in regions I and II instead of the corresponding potential representations as is the case of the last matching step followed in [16]. This is effectively what has been carried out in [17].

In the latter work the author also finds that the associated viscous motion arising near the corner walls is characterized by five distinct boundary layer regions (reduced to three in view of symmetry) as shown in Fig. 2, namely a corner layer (region (i)) separated by an intermediate viscous layer (region (iii)) from the far-field boundary layers (regions (ii)) on each of its sides; all of these layers exhibit three-dimensional motions but with different degrees of strength.

To investigate combined free and forced convection viscous motion, we find it convenient to work with non-dimensional flow variables. To this end let (u, v, w) designate the primitive velocity vector associated to the Cartesian directions (x, y, z), p be the fluid pressure and T be its temperature. Then, in order to analyse the different flow regions as well as various mixed-convection situations we introduce the following mappings of the flow variables

$$\begin{aligned} &(u, v, w) \mapsto U_\infty(\varepsilon_x u, \varepsilon_y v, w), \quad p + \rho_\infty g^* z_g \mapsto \rho_\infty U_\infty^2 p, \\ &(x, y, z) \mapsto l(\delta_x x, \delta_y y, z), \quad T \mapsto \frac{T - T_\infty}{\Delta T}, \end{aligned} \tag{2.7}$$

in which z_g is a vertical ascendant Cartesian coordinate, ΔT is a temperature difference scale, T_∞ and ρ_∞ are, respectively, the undisturbed fluid temperature and density, and g^* is the gravitational acceleration. The orders of magnitude of the gauge parameters $\varepsilon_x, \varepsilon_y, \delta_x$ and δ_y are determined according to the flow region under consideration such that the non-dimensional quantities (u, v, w) remain O(1). Inserting the above definitions into the continuity, Navier–Stokes and energy equations yields after carrying out the Boussinesq approximations the following non-dimensional equations

$$\frac{\varepsilon_x}{\delta_x}\frac{\partial u}{\partial x} + \frac{\varepsilon_y}{\delta_y}\frac{\partial v}{\partial y} + \frac{\partial w}{\partial z} = 0, \tag{2.8}$$

$$\begin{aligned} &\frac{\varepsilon_x^2}{\delta_x}u\frac{\partial u}{\partial x} + \frac{\varepsilon_x\varepsilon_y}{\delta_y}v\frac{\partial u}{\partial y} + \varepsilon_x w\frac{\partial u}{\partial z} \\ &\quad = -\frac{1}{\delta_x}\frac{\partial p}{\partial x} + \frac{Gr}{Re^2}\lambda_x T \\ &\qquad + \frac{\varepsilon_x}{\delta_y^2 Re}\left(\frac{\delta_y^2}{\delta_x^2}\frac{\partial^2 u}{\partial x^2} + \frac{\partial^2 u}{\partial y^2} + \delta_y^2\frac{\partial^2 u}{\partial z^2}\right), \end{aligned} \tag{2.9}$$

$$\begin{aligned} &\frac{\varepsilon_x\varepsilon_y}{\delta_x}u\frac{\partial v}{\partial x} + \frac{\varepsilon_y^2}{\delta_y}v\frac{\partial v}{\partial y} + \varepsilon_y w\frac{\partial v}{\partial z} \\ &\quad = -\frac{1}{\delta_y}\frac{\partial p}{\partial y} + \frac{Gr}{Re^2}\lambda_y T \\ &\qquad + \frac{\varepsilon_y}{\delta_y^2 Re}\left(\frac{\delta_y^2}{\delta_x^2}\frac{\partial^2 v}{\partial x^2} + \frac{\partial^2 v}{\partial y^2} + \delta_y^2\frac{\partial^2 v}{\partial z^2}\right), \end{aligned} \tag{2.10}$$

$$\begin{aligned} &\frac{\varepsilon_x}{\delta_x}u\frac{\partial w}{\partial x} + \frac{\varepsilon_y}{\delta_y}v\frac{\partial w}{\partial y} + w\frac{\partial w}{\partial z} \\ &\quad = -\frac{\partial p}{\partial z} + \frac{Gr}{Re^2}\lambda_z T + \frac{1}{\delta_y^2 Re}\left(\frac{\delta_y^2}{\delta_x^2}\frac{\partial^2 w}{\partial x^2} + \frac{\partial^2 w}{\partial y^2} + \delta_y^2\frac{\partial^2 w}{\partial z^2}\right), \end{aligned} \tag{2.11}$$

$$\frac{\varepsilon_x}{\delta_x}u\frac{\partial T}{\partial x}+\frac{\varepsilon_y}{\delta_y}v\frac{\partial T}{\partial y}+w\frac{\partial T}{\partial z}$$
$$=\frac{1}{PrRe\delta_y^2}\left(\frac{\delta_y^2}{\delta_x^2}\frac{\partial^2 T}{\partial x^2}+\frac{\partial^2 T}{\partial y^2}+\delta_y^2\frac{\partial^2 T}{\partial z^2}\right). \quad (2.12)$$

Here $(\lambda_x,\lambda_y,\lambda_z)$ are the direction cosines made by the z_g-direction with the (x,y,z)-directions, $Gr=\beta^* g^* l^3\Delta T/\nu^2$ and $Pr=\nu/\kappa^*$ are, respectively, the Grashof and Prandtl numbers, in which β^* denotes the coefficient of thermal expansion and κ^* is the fluid thermal diffusivity. In what follows the Reynolds number Re will be assumed to be sufficiently large to use boundary layer approximations. For the boundary conditions we impose first the wall no-slip condition for the velocity vector together with either a prescribed wall temperature or a prescribed wall heat flux. Second, conditions on the velocity components at the outer reaches of the boundary layer are deduced from the matching requirements with the potential flow while for the temperature field we have $T=0$. Third, conditions in the x-direction must allow for smooth merger between adjacent layers. Observe that as one moves (in the x-direction) away from the corner line towards the consecutive boundary layers, the order of length and velocity gauge parameters change and so will the flow properties. Consequently, different flow characteristics prevail in the different regions with crucial differences arising between convex and concave corner flow configurations (see Section 4.3). Note also that since the boundary layer at the inner limit of region (ii) constitutes a boundary condition for region (iii), its treatment will not be considered separately for it is implicitly included in that of the latter region.

From the outset, but without much loss of generality, attention will exclusively be focused in what follows on almost planar corners for which corner flow properties arise when $\alpha=O(1/\ln Re)$ as shown by Smith [19] for the special case of three-dimensional stagnation flow into a corner and by Ridha [17] for corner flow with an arbitrary streamwise pressure gradient. Furthermore, for brevity and due to lack of space only numerical results pertaining to fixed wall temperature distribution are presented herein, throughout the Prandtl number has been set to unity. Finally, because of symmetry attention is confined to the quarter-infinite space $(x,y)\geqslant 0$, $z>0$. With this in mind, we start below by deriving boundary-layer equations for region (iii) before considering flow properties thereat.

3. The intermediate layer, region (iii)

We have for this layer $\delta_x=\delta$, $\varepsilon_x=\delta/\ln Re$, $\varepsilon_y=Re^{-1/2}$ which lead, to the leading order in Re, to the following boundary-layer equations

$$\frac{\partial v}{\partial y}+\frac{\partial w}{\partial z}=0, \quad (3.1)$$

$$v\frac{\partial u}{\partial y}+w\frac{\partial u}{\partial z}=-\left(\frac{\ln Re}{\delta^2}\right)\frac{\partial p}{\partial x}+f_x T+\frac{\partial^2 u}{\partial y^2}, \quad (3.2)$$

$$\frac{\partial p}{\partial y}=f_y T, \quad (3.3)$$

$$v\frac{\partial w}{\partial y}+w\frac{\partial w}{\partial z}=-\frac{\partial p}{\partial z}+f_z T+\frac{\partial^2 w}{\partial y^2}, \quad (3.4)$$

$$v\frac{\partial T}{\partial y}+w\frac{\partial T}{\partial z}=\frac{1}{Pr}\frac{\partial^2 T}{\partial y^2}, \quad (3.5)$$

in which

$$f_x=\left(\frac{Gr\ln Re}{\delta Re^2}\right)\lambda_x,\quad f_y=\left(\frac{Gr}{Re^{5/2}}\right)\lambda_y,$$
$$f_z=\left(\frac{Gr}{Re^2}\right)\lambda_z. \quad (3.6)$$

These equations together with the potential flow suggest setting

$$p(x,y,z)=p_0(z)+p_1(y,z)+\left(\frac{\delta^2}{\ln Re}\right)p_2(x,z)$$
$$+\cdots \quad (3.7)$$

Equations (3.2)–(3.7) offer extremely large number of possibilities related to the orientation of the corner walls with respect to the gravitational force. For instance, a corner with one wall kept horizontal gives rise to asymmetrical flow in general. Nevertheless, for almost planar corners the flow exhibits (to the leading order of approximation) symmetry with respect to the corner bisector plane. Hence, such a case is characterized by $(f_x,f_z)\sim 0$, $f_y\sim Gr/Re^{5/2}$ and consequently the buoyancy effect on the crossflow is indirect and takes place mainly through its interaction with the primary flow component. For an almost vertical corner walls with a horizontal corner line on the other hand, the buoyancy force is felt (again to the leading order of approximations) by the secondary flow only, the primary flow motion remaining as that past a wedge with no heat transfer. For such a situation we have $f_x\sim Gr\ln Re/\delta Re^2$, $f_y\ll Gr/Re^{5/2}$, $f_z\ll Gr/Re^2$ since $\lambda_x\sim 1$, $(\lambda_y,\lambda_z)\ll 1$ and $1\gg\delta\gg Re^{-1/2}$. On the other hand when the corner line is almost vertical $(f_x,f_y)\sim 0$, $f_z\sim Gr/Re^2$ and so thermal convection influences the primary and secondary flows in a similar fashion as that indicated for the first example. Presumably, the most interesting situation is that where the corner is so oriented that $(f_x,f_y,f_z)\sim O(Gr/Re^{5/2})$ which can be obtained if $\lambda_x\sim O(\delta Re^{-1/2}/\ln Re)$, $\lambda_y\sim 1$, $\lambda_z\sim O(Re^{-1/2})$. For this configuration there is, unfortunately, no similarity-type formulation and Eqs. (3.2)–(3.5), subject to appropriate boundary conditions, must then be solved numerically. This is beyond the object of the present paper which is confined only to situations leading to

similarity-type solutions. For such a situation, it can be shown that the temperature is essentially a function of (y,z) only (to the leading order of approximations). For brevity we shall then consider only flows along corners having almost horizontal walls problem where $(f_x,f_z)\ll f_y$. In such a case Eqs. (3.2)–(3.5) reduce to those corresponding to a mixed-convection boundary layer flow over a horizontal surface with a cross flow given by (2.1), and as a consequence we find from (3.3)

$$p_1(y,z)=p_1(y=\infty,z)-\int_y^\infty f_yT\,\mathrm{d}y. \tag{3.8}$$

Given that the resulting equations admit similarity-type solutions, we introduce the following variable transformations

$$\psi=cz^{(1+m)/2}\left[h(\eta)+\frac{K}{\ln Re}h_1(\xi,\eta)+\cdots\right], \tag{3.9}$$

$$u=\frac{2m}{\pi}K\xi(\ln\xi-1)z^{(m-1)/2}\left[g(\xi,\eta)+\frac{K}{\ln Re}g_1(\xi,\eta)+\cdots\right], \tag{3.10}$$

$$T=z^q\left[\theta(\eta)+\frac{K}{\ln Re}\theta_1(\xi,\eta)+\cdots\right], \tag{3.11}$$

where $c=\sqrt{2/m+1}$, $v=-\partial\psi/\partial x$, $w=\partial\psi/\partial y$, and $(x,y)=cz^{(1-m)/2}(\xi,\eta)$ which implies that the intermediate layer is now defined by $\xi\in[0,1]$. For the pressure term, we find $p_2=-m(m-1)Kz^{m-1}\xi^2(\ln\xi-1)/\pi$ upon using the potential flow conditions. Note that to have constant wall temperature we must set $q=(5m-1)/2$. Inserting these definitions into Eqs. (3.2)–(3.5) yields

$$g''+hg'+\gamma(\xi)(\beta-1)(1-h'g)=\xi(\beta-1)h'\frac{\partial g}{\partial\xi}, \tag{3.12}$$

$$h'''+hh''+\beta(1-h'^2)+\sigma(2-\beta)^{1/2}\times\left\{2\beta\int_\eta^\infty\theta(\zeta)\,\mathrm{d}\zeta+(1-\beta)\eta\theta\right\}=0, \tag{3.13}$$

$$\frac{1}{Pr}\theta''+h\theta'-(3\beta-1)h'\theta=0, \tag{3.14}$$

where $\gamma(\xi)=(2\ln\xi-1)/(\ln\xi-1)$, and $\sigma=f_y$ which will henceforth be referred to as the buoyancy parameter. The appropriate boundary conditions are

$$h(0)=h'(0)=g(.,0)=0,\quad \theta(0)=1 \tag{3.15}$$

for a prescribed wall temperature, together with

$$h'(\infty)=g(.,\infty)=1,\quad \theta(\infty)=0 \tag{3.16}$$

at the outer reaches of the boundary layer. Conditions at the outer limit of the intermediate layer are obtained by solving (3.12) when

$$\lim_{\xi\to1}\frac{\partial g}{\partial\xi}\to0. \tag{3.17}$$

Equations (3.13) and (3.14) are basically the same as those studied in [20] for mixed convection boundary layer flow over a horizontal surface, and are characterized by their non-uniqueness in the (β,σ)-space.

System (3.12)–(3.14) subject to (3.15)–(3.17) has been numerically solved for constant wall temperature ($\beta=1/3$), and results for the crossflow velocity and streamwise vorticity are presented in Figs. 3 and 4. In Fig. 3, it is seen that the crossflow exhibits a flow reversal which becomes more pronounced for opposing flows ($\sigma<0$) than for aiding flows ($\sigma>0$); as illustrated in Fig. 4, this reflects the existence of a closed streamwise vortex described by $-2m\xi(\ln\xi-1)g'/\pi c$. As predicted by Moore [18] and recently confirmed by the author [17], such results show that a system of two symmetrically disposed vortices proceed from the forward corner; they arise from the generation of transverse circulation specifically in the intermediate layer, region (iii), and not in the corner layer as was first predicted. Their position and strength vary with the pressure gradient and the corner angle, namely the exponent m and K in the present situation. Figs. 3 and 4 illustrate therefore the vortex behaviour under the influence of combined free and forced convection; for $\sigma<0$ the vortex moves towards the inner limit of region (iii) with decreasing σ, the reverse flow region occupying now an important part of the boundary layer. On the other hand, with increasing $\sigma>0$ the vortex drifts outward towards region (ii), the reverse flow regions becoming now smaller and eventually disappearing from region (iii) for $\sigma\geqslant3$. The inverse prevails of course for a flow along a corner the surface of which is facing downwards. Hence, insofar as the intermediate layer is concerned, it may be inferred that for a flow along a horizontal corner the surface of which is facing upward heating would enhance flow stability, whilst cooling would be required to achieve the same effect when the said surface is facing downwards.

4. The corner layer, region (i)

In view of symmetry with respect to the corner bisector plane we have here $\delta_x=\delta_y$, $\varepsilon_x=\varepsilon_y$. For almost planar corners we find from continuity considerations and matching requirements with the potential flow that $\delta_x=\varepsilon_x=\delta_y=\varepsilon_y=Re^{-1/2}$. Accordingly the boundary layer equations become

$$\frac{\partial u}{\partial x}+\frac{\partial v}{\partial y}+\frac{\partial w}{\partial z}=0, \tag{4.1}$$

$$u\frac{\partial u}{\partial x}+v\frac{\partial u}{\partial y}+w\frac{\partial u}{\partial z}=-Re\frac{\partial p}{\partial x}+Ref_xT+\frac{\partial^2u}{\partial x^2}+\frac{\partial^2u}{\partial y^2}, \tag{4.2}$$

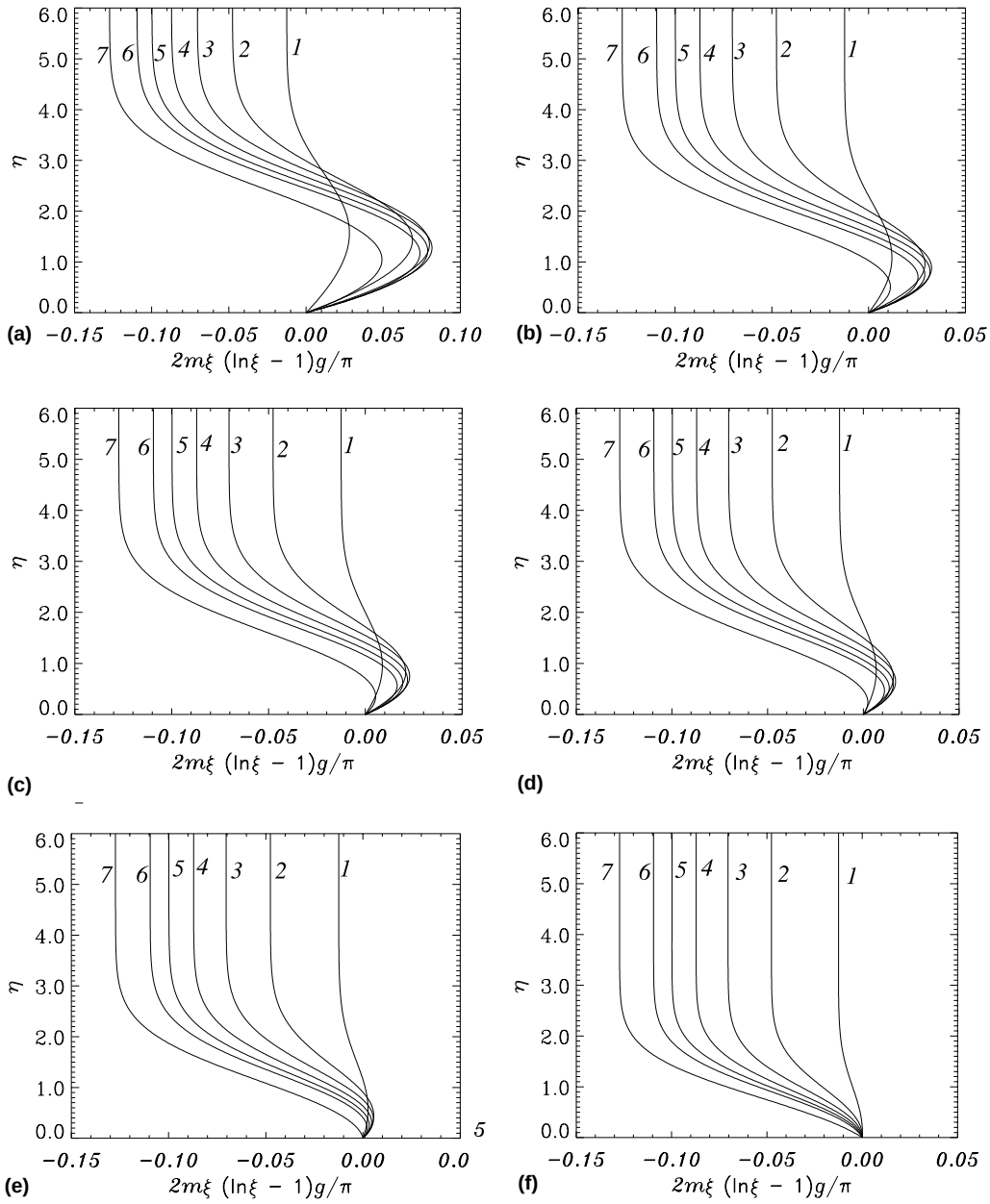

Fig. 3. Crossflow velocity profiles in region (ii) for constant wall temperature condition, $\beta = 1/3$. Figs. (a)–(f) correspond to $\sigma = -0.47, -0.2, 0.0, 0.2, 1.0, 3.0$, the first value pertaining to a primary flow having a separation profile, $h''(0) = 0$. Curves 1–7 correspond to $\xi = 0.02, 0.12, 0.22, 0.32, 0.42, 0.52, 1.0$.

$$u\frac{\partial v}{\partial x} + v\frac{\partial v}{\partial y} + w\frac{\partial v}{\partial z} = -Re\frac{\partial p}{\partial y} + Ref_y T + \frac{\partial^2 v}{\partial x^2} + \frac{\partial^2 v}{\partial y^2}, \tag{4.3}$$

$$u\frac{\partial w}{\partial x} + v\frac{\partial w}{\partial y} + w\frac{\partial w}{\partial z} = -\frac{\partial p}{\partial z} + f_z T + \frac{\partial^2 w}{\partial x^2} + \frac{\partial^2 w}{\partial y^2}, \tag{4.4}$$

$$u\frac{\partial T}{\partial x} + v\frac{\partial T}{\partial y} + w\frac{\partial T}{\partial z} = \frac{1}{Pr}\left(\frac{\partial^2 T}{\partial x^2} + \frac{\partial^2 T}{\partial y^2}\right) \tag{4.5}$$

in which $(f_x, f_y) = (\lambda_x, \lambda_y)Gr/Re^{5/2}$ and $f_z = Gr\lambda_z/Re^2$.

Equations (4.1)–(4.5) are to be solved subject first to the no-slip condition together with an appropriate thermal condition on the body surface. Second, to ensure smooth merger with the inner limits of the intermediate layers pertinent boundary conditions are to be derived in general. Finally, in order to account for the displacement effect on the potential flow the matching conditions with the inviscid flow may be casted in the following form

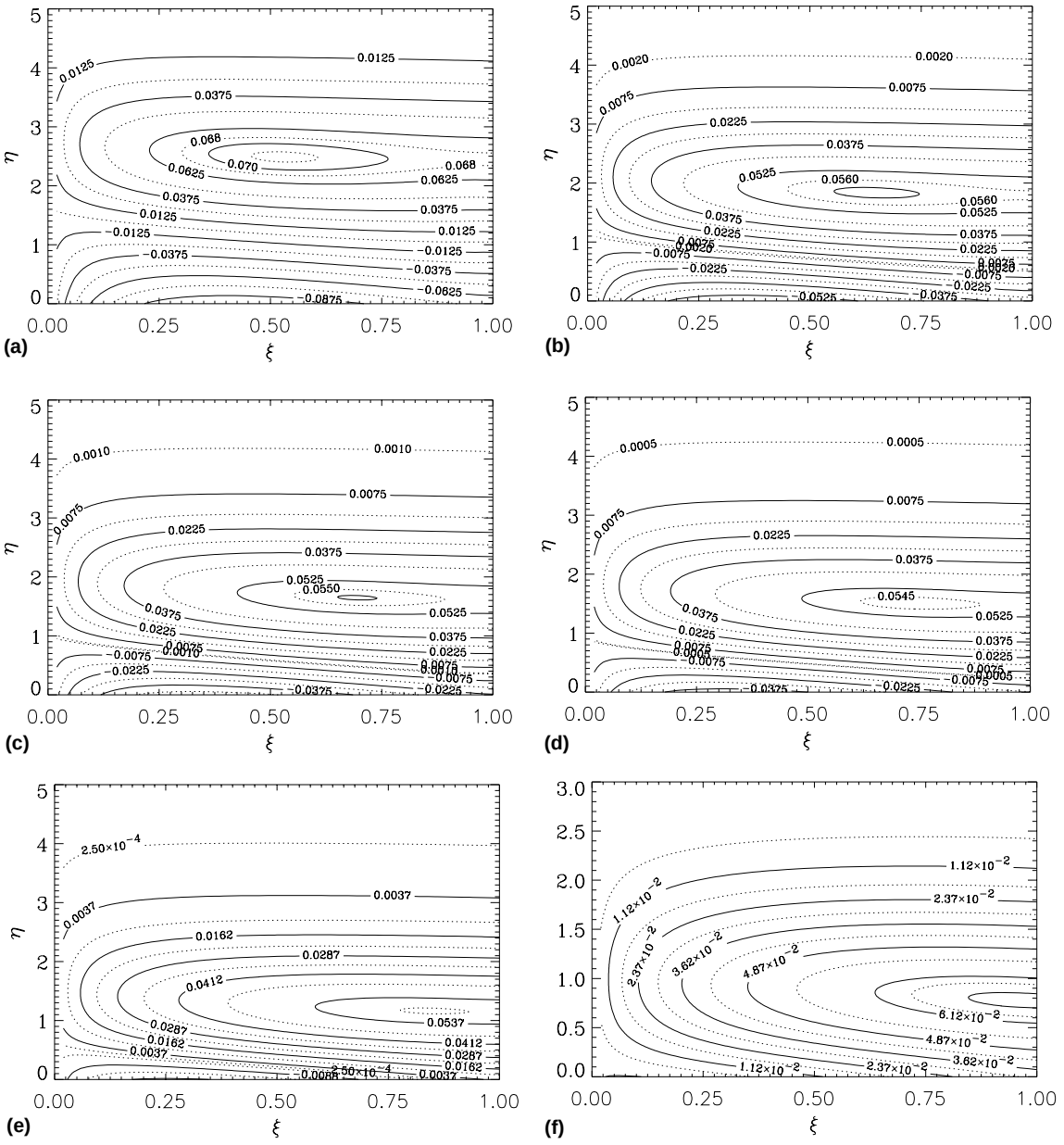

Fig. 4. Constant streamwise vorticity contours in region (ii) for constant wall temperature condition, $\beta = 1/3$. Figs. (a)–(f) correspond to $\sigma = -0.47, -0.2, 0.0, 0.2, 1.0, 3.0$.

$$\begin{aligned}
\frac{\partial u}{\partial x} &= -\frac{1}{2} m z^{m-1} \delta_x \varepsilon_x^{-1} \\
&\quad \times \left[1 - \mathscr{U} z^{(s-2)(m-1)/2} r^{s-2} \cos(s-2)\vartheta\right], \\
\frac{\partial v}{\partial y} &= -\frac{1}{2} m z^{m-1} \delta_y \varepsilon_y^{-1} \\
&\quad \times \left[1 + \mathscr{U} z^{(s-2)(m-1)/2} r^{s-2} \cos(s-2)\vartheta\right], \\
w &= z^m
\end{aligned} \tag{4.6}$$

in which we have set $\delta \sim Re^{-1/M}$, $M > 2$ since $1 \gg \delta \gg Re^{-1/2}$. When $s \to 2$ we find

$$\begin{aligned}
&s - 2 \sim \frac{4\alpha}{\pi}\left(1 + \frac{2\alpha}{\pi}\right), \quad \mathscr{U} \sim \left(1 - \frac{4K\alpha}{\pi^2}\right)\exp(-2K/\pi), \\
&\alpha = \frac{K}{\ln Re}, \quad K \mapsto \frac{K(M-2)}{M}, \quad K \sim 1.
\end{aligned} \tag{4.7}$$

In deriving conditions (4.6) from (2.1)–(2.3), only terms in $(\delta^*/\delta)^{s-2}$ are approximated, recall that δ^* refers to the corner layer thickness (see Fig. 2) which is in fact equal to δ_x in this case.

To obtain similarity solutions of the boundary layer equations the following conformal transformation

$$\begin{aligned} &r\exp(\mathrm{i}\vartheta) = cz^{(1-m)/2}\rho^n\exp(\mathrm{i}n\chi), \quad n = 2/s,\\ &(\xi,\eta) = \rho(\cos\chi,\sin\chi) \end{aligned} \tag{4.8}$$

is employed followed by eliminating the pressure gradients terms in the x- and y-directions upon using the streamwise vorticity equation, the body surface is defined now by $\eta = 0$. Accordingly we seek solutions in the form

$$\begin{aligned} u &= -Z\big\{J^{-1/2}[F\cos(\vartheta-\chi) - G\sin(\vartheta-\chi)]\\ &\quad + (\beta-1)\rho^n H\cos\vartheta\big\},\\ v &= -Z\big\{J^{-1/2}[F\sin(\vartheta-\chi) + G\cos(\vartheta-\chi)]\\ &\quad + (\beta-1)\rho^n H\sin\vartheta\big\},\\ w &= z^m H, \quad \frac{T-T_\infty}{T_\mathrm{w}-T_\infty} = z^q\theta,\\ p &= \frac{1}{2}z^{2m}\left(-1 + p^*(\xi,\eta;Gr,Re)\right), \end{aligned} \tag{4.9}$$

where (F,G,H,θ) are functions of $(\xi,\eta;Gr,Re)$, with $J = n^2\rho^{2(n-1)}$ and $Z = c^{-1}z^{(m-1)/2}$. Substituting these definitions into the boundary-layer equations for this region we find after some manipulations that

$$\frac{\partial F}{\partial\xi} + \frac{\partial G}{\partial\eta} - (2-\beta)JH = 0, \tag{4.10}$$

$$\triangle H + F\frac{\partial H}{\partial\xi} + G\frac{\partial H}{\partial\eta} + J\beta(1-H^2) - \beta Jp^* + \mathscr{A}\theta = 0, \tag{4.11}$$

$$\begin{aligned} \triangle\omega + F\frac{\partial\omega}{\partial\xi} + G\frac{\partial\omega}{\partial\eta} + JH\Big[&(2-\beta)\omega + s(1-\beta)\\ &\times\left(\eta\frac{\partial H}{\partial\xi} - \xi\frac{\partial H}{\partial\eta}\right)\Big] + \mathscr{B} = 0, \end{aligned} \tag{4.12}$$

$$\frac{1}{Pr}\triangle\theta + F\frac{\partial\theta}{\partial\xi} + G\frac{\partial\theta}{\partial\eta} - c^2JqH\theta = 0 \tag{4.13}$$

coupled to the modified vorticity definition

$$\omega = \left(\frac{\partial F}{\partial\eta} - \frac{\partial G}{\partial\xi}\right)/J \tag{4.14}$$

and the reduced Laplacian operator

$$\triangle = \frac{\partial^2}{\partial\xi^2} + \frac{\partial^2}{\partial\eta^2}.$$

In Eqs. (4.11) and (4.12) we have

$$\begin{aligned} \mathscr{A} &= \frac{Gr}{Re^{5/2}}(2-\beta)^{1/2}(1-\beta)\big(\lambda_x\cos\vartheta + \lambda_y\sin\vartheta\big)\\ &\quad\times J\rho^n z^{q+(1-5m)/2} + \frac{Gr}{Re^2}(2-\beta)J\lambda_z z^{q+1-2m}, \end{aligned} \tag{4.15}$$

$$\begin{aligned} \mathscr{B} &= \frac{Gr}{Re^{5/2}}\mu c^5 J\left(\frac{1-m}{2}\right)\rho^n\big(\lambda_x\sin\vartheta - \lambda_y\cos\vartheta\big)\\ &\quad\times\left\{q\theta - \mu\left(\eta\frac{\partial\theta}{\partial\eta} + \xi\frac{\partial\theta}{\partial\xi}\right)\right\}z^{q+(1-5m)/2}\\ &\quad + \frac{Gr}{Re^2}c^4\mu J\lambda_z\left(\xi\frac{\partial\theta}{\partial\eta} - \eta\frac{\partial\theta}{\partial\xi}\right)z^{q+1-2m}\\ &\quad - \frac{Gr}{Re^{3/2}}c^3J^{1/2}\left\{\big(\lambda_x\cos(\vartheta-\chi) + \lambda_y\sin(\vartheta-\chi)\big)\frac{\partial\theta}{\partial\eta}\right.\\ &\quad\left. + \big(\lambda_x\sin(\vartheta-\chi) - \lambda_y\cos(\vartheta-\chi)\big)\frac{\partial\theta}{\partial\xi}\right\}z^{q+3(1-m)/2} \end{aligned} \tag{4.16}$$

in which $\mu = (1-m)/2n$. Eqs. (4.10)–(4.14) are to be solved subject to the wall conditions

$$\eta = 0; \quad F = G = H = 0, \quad \theta = 1, \tag{4.17}$$

in addition to the inviscid flow matching requirements as $\eta\to\infty$. For $\alpha = \mathrm{O}(1/\ln Re)$ these become

$$\begin{aligned} &\frac{\partial F}{\partial\xi}\sim 1 - \frac{1}{2}\beta(1+\exp(-2K/\pi)) + \mathrm{O}(\alpha), \quad H\to 1,\\ &\frac{\partial G}{\partial\eta}\sim 1 - \frac{1}{2}\beta(1-\exp(-2K/\pi)) + \mathrm{O}(\alpha), \quad \omega\to 0. \end{aligned} \tag{4.18}$$

Clearly conditions (4.18) suggest that we can look for solutions in the form

$$\begin{aligned} (F,G,H,\omega,p^*,\theta) &= (\xi F_0, G_0, H_0, \xi\omega_0, p_0, \theta_0)\\ &\quad + (F_1,G_1,H_1,\omega_0,p_1,\theta_1)/\ln Re\\ &\quad + \cdots \end{aligned} \tag{4.19}$$

at this limit, where $(F_0,G_0,H_0,\omega_0,p_0,\theta_0)$ are functions of η only whilst $(F_1,G_1,H_1,\omega_0,p_1,\theta_1)$ are functions of (ξ,η). Now since for almost planar corners having nearly horizontal walls $n\to 1$, $(\lambda_x,\lambda_z)\ll\lambda_y\sim 1$, then we find

$$\begin{aligned} &\mathscr{A}\sim\sigma(2-\beta)^{1/2}(1-\beta)\eta,\\ &\mathscr{B}\sim\sigma(2-\beta)^{1/2}(1-\beta)\xi\left\{(1-\beta)\eta\frac{\partial\theta_0}{\partial\eta} - (3\beta-1)\theta_0\right\} \end{aligned} \tag{4.20}$$

after setting $q = (5m-1)/2$, where the buoyancy parameter is defined by $\sigma = Gr/Re^{5/2}$. Inserting definitions (4.20) and solutions (4.19) into Eqs. (4.11)–(4.14) yields

$$F_0 + G_0' - (2-\beta)H_0 = 0, \tag{4.21}$$

$$H_0'' + G_0H_0' + \beta(1-H_0^2) - \beta p_0 + \sigma(2-\beta)^{1/2}(1-\beta)\eta\theta_0 = 0, \tag{4.22}$$

$$\begin{aligned} \omega_0'' + F_0\omega_0 + G_0\omega_0' + H_0\big[&(2-\beta)\omega_0 - 2(1-\beta)H_0'\big]\\ &+ \sigma(2-\beta)^{1/2}(1-\beta)\Big[(1-\beta)\eta\theta_0' - (3\beta-1)\theta_0\Big] = 0, \end{aligned} \tag{4.23}$$

$$\frac{1}{Pr}\theta_0'' + G_0\theta_0' - (3\beta - 1)H_0\theta_0 = 0, \tag{4.24}$$

$$\omega_0 = F_0' \tag{4.25}$$

to the leading order in Re, in which a prime denotes differentiation with respect to η. To determine p_0 for an almost planar corner flow, we must consider the momentum equation in the η-direction in exactly the same manner as in [21] for the free convection problem from a horizontal plate. We find

$$p_0 = -2\sigma(2-\beta)^{1/2}\int_\eta^\infty \theta_0(\zeta)\,\mathrm{d}\zeta. \tag{4.26}$$

when $n \to 1$. Equations (4.22)–(4.26) are to be solved then subject to the wall no-slip condition $F_0(0) = G_0(0) = H_0(0) = 0$ together with $\theta(0) = 1$, and $F_0(\infty) = 1 - \beta(1 + \exp(-2K/\pi))/2$, $H_0(\infty) = 1$, $\omega_0(\infty) = 0$ at the outer limit of the boundary layer. Solutions of these equations are characterized by their non-uniqueness in the (β, σ, K)-space and so we shall for convenience refer to those solutions having the higher value of $H_0'(0)$ as the upper branch solution when $\beta = 1/3$, $\sigma = 0$. Apart from the condition on $F_0(\infty)$, it is worth noting that the above equations and conditions are in fact essentially the same as those corresponding to the mixed convection boundary layer problem over a horizontal surface in the vicinity of a plane of symmetry treated in [22]. Indeed, this problem is recovered when $K \to \infty$ which suggests that in spite of having Eqs. (4.22)–(4.26) derived for $K \sim 1$, it remains nevertheless very instructive to look into their properties for large values of $|K|$ as shown by Smith [19] for the three-dimensional flow stagnation point flow into a corner, or by Ridha [17] for the general corner flow problem. First, when $\alpha = \mathrm{O}(1)$ and positive, $K \to \infty$ and so the obtained equations and boundary conditions correspond in fact to boundary conditions for the corner layer proper (this can easily be shown in considering the full corner layer problem) when ξ is large in the case of concave corners. (See [17] for the corresponding problem with no heat transfer.) For convex corners on the other hand, $\alpha = \mathrm{O}(1)$ and negative $K \to -\infty$. We shall therefore consider in what follows properties of Eqs. (4.22)–(4.26) according to the order of magnitude of K.

4.1. $K \ll 1$

For small K we can formally look for solutions in the following form

$$(F_0, G_0, H_0, \theta_0) \mapsto (F_0, G_0, H_0, \theta_0) + K(F_1, G_1, H_1, \theta_1) + \mathrm{O}(K^2). \tag{4.27}$$

Clearly $(F_0, G_0, H_0, \theta_0)$ is a solution of Eqs. (4.22)–(4.26) but subject to $F_0(0) = G_0(0) = H_0(0) = 0$, $\theta_0(0) = 1$ and $F_0(\infty) = 1 - \beta$, $H_0(\infty) = 1$, $\theta_0(\infty) = 0$. Moreover, it can easily be verified that these equations are satisfied by $F_0 = (1-\beta)H_0$ which is a solution of Eqs. (3.13) and (3.14) but with $G_0 = h$, $H_0 = h'$ and $\theta_0 = \theta$. Note that this solution implies $u = 0$ to the zeroth order in K and so, the problem corresponds in this situation to a primary mixed convection flow past a horizontal surface but with a small perturbation accounting for the crossflow, the primary flow problem becoming now basically that treated in [20].

The perturbation solution is described by the following system of equations

$$H_1'' + G_0H_1' + G_1H_0' - 2\beta H_0H_1 + \sigma(2-\beta)^{1/2} \times \left[2\beta\int_\zeta^\infty \theta_1(\zeta)\,\mathrm{d}\zeta + (1-\beta)\eta\theta_1\right] = 0, \tag{4.28}$$

$$F_1'' + G_0F_1' + (1-\beta)G_1H_0' + 2(1-\beta)H_0(F_1 - H_1) + \sigma(2-\beta)^{1/2}(1-\beta)\left[2\beta\int_\zeta^\infty \theta_1(\zeta)\,\mathrm{d}\zeta + (1-\beta)\eta\theta_1\right] = 0, \tag{4.29}$$

$$\frac{1}{Pr}\theta_1'' + G_0\theta_1' + G_1\theta_0' - (3\beta - 1)[\theta_1H_0 + \theta_0H_1] = 0, \tag{4.30}$$

$$F_1 + G_1' - (2-\beta)H_1 = 0 \tag{4.31}$$

subject to $F_1(0) = G_1(0) = H_1(0) = 0$, $\theta_1(0) = 0$ at the wall. Conditions at the outer reaches of the boundary layer are $F_1(\infty) = \beta/\pi$, $H_1(\infty) = \theta_1(\infty) = 0$.

Setting

$$u = Z(u_0 + Ku_1 + \cdots), \quad w = z^m(w_0 + Kw_1 + \cdots) \tag{4.32}$$

enables us to present the numerical results in terms of (u_1, w_1) as shown in Fig. 5, in which Fig. 5(a),(c),(e) depict, respectively, the behaviour of $(w_1', u_1', \theta_1')(0)$ with varying σ. Here it is observed that the lower branch solution in the interval $-0.0 > \sigma > -0.471$ exhibits four singularity points, where u_1 changes its direction near the wall. However, this is of no physical significance since in this interval $w_0'(0) < 0$ which implies that this part of the solution does not in fact represent a correct mathematical model of a separated flow; see in this connection [23], for instance. In contrast, results for which $w_0'(0) \geqslant 0$ do bear some physical interest, particularly for u_1. For $\sigma \leqslant 4.0$ the crossflow components u_1 exhibits a flow reversal whilst for $\sigma > 4.0$ it is seen to be completely directed towards the symmetry plane. Hence it would be interesting to look into the secondary flow instabilities in such a situation, a question that is again beyond the purpose of the present paper.

Consideration of the numerical results presented so far shows that, to leading orders, the link is assured for the primary and secondary flows alike between the corner and intermediates layers. The most striking

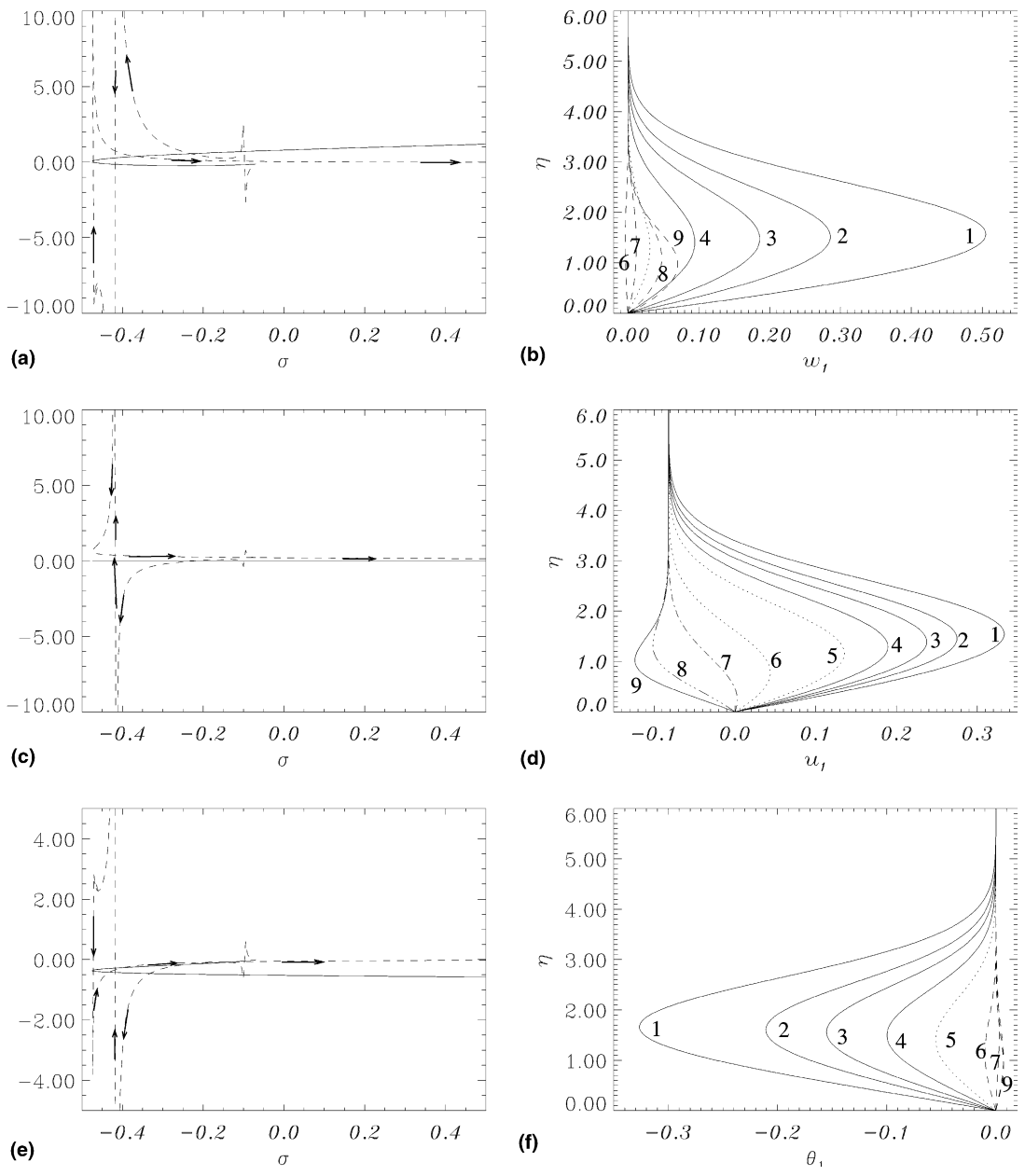

Fig. 5. Falkner–Skan branch solution; in figures (a),(c),(e) solid lines correspond to $w_0'(0), u_0'(0), \theta_0'(0)$ and broken lines to $w_1'(0), u_1'(0), \theta_1'(0)$ with arrows designating changes of σ from −0.0 on the lower branch towards the turning critical point −0.471 and then in the sense of increasing σ thereafter. In (b),(d),(f) curves 1–9 correspond to $\sigma = -0.4, -0.35, -0.3, -0.2, 0.0, 1.0, 3.0, 10.0, 20.0$, respectively.

feature in these results is certainly how an infinitesimal cranking in an otherwise plane surface (in the corner geometry sense) can give rise to such a complex and rich behaviour of the secondary flow, this is rather surprising and somewhat unexpected. When $K \sim 1$ such an effect of an almost planar corner on the boundary layer flow becomes more pronounced as will shortly be seen below.

In addition to the foregoing perturbation solution, there exists however another one for which $u_0 \neq 0$ to the zeroth order in K. It is precisely for this reason that the link with the boundary-layer solution in region (iii) is not assured since u is O(1) now according to (4.32). Effectively, this solution corresponds to a mixed convection boundary layer flow over a horizontal surface in

the neighbourhood of a plane of symmetry, and the author is of the opinion that it does not correspond to a corner layer solution. Following this reasoning and due to lack of space, corresponding results are not presented herein. Moreover, a somewhat similar boundary flow problem in the vicinity of a symmetry plane has already been examined in [22].

4.2. $K \sim 1$

For constant wall temperature ($\beta = 1/3$), solutions of Eqs. (4.22)–(4.26) are only found for $K > 0$ and O(1), that is for concave corners only. This is clearly shown in Fig. 6(a) which depicts the behaviour of $u'(0), w'(0), \theta'(0)$ versus K according to the mappings $u \mapsto Z\xi u$, $H_0 \mapsto w$, $\theta_0 \mapsto \theta$, compare with definitions (4.9) and (4.19). In general, for each value of K two solutions are found when $\sigma \geqslant 0$ and four when $\sigma < 0$. Now since K appears in the form $\exp(-2K/\pi)$, we find it convenient to keep $\exp(-2K/\pi) \sim 1$ in order to better discern the effect of the corner angle on the boundary layer flow in this range. To this end we have chosen $K = 3$ and results are presented in Figs. 6(b)–(d) and 7. Again, the most striking feature here is the crossflow behaviour particularly when the primary flow displays a separation profile as shown in Fig. 6(d) (curve 1) and Fig. 7(a). For this particular case, the crossflow in the vicinity of the wall is seen to drift away from the plane of symmetry for both the upper and lower branches. On the other hand, sufficiently far from the body surface the crossflow (corresponding to the upper branch solution) exhibits a complex flow pattern. In the upper reaches of the corner layer it drifts inward towards the symmetry plane whilst executing a U-turn like behaviour midway within the boundary layer; this behaviour, when coupled to results obtained for the intermediate layer, suggests that the link with region (ii) is assured. For the lower branch solution the behaviour of the crossflow is considerably less complex. As σ is increased, the crossflow undergoes more changes in the case of the lower branch solution than in the upper one. Again, numerical results show that the slightest bending (in a streamwise corner geometry sense) of an otherwise plane surface could leads to a rich and varied crossflow behaviour, with perhaps an important effect on the flow stability, in particular with regards to secondary flow instabilities.

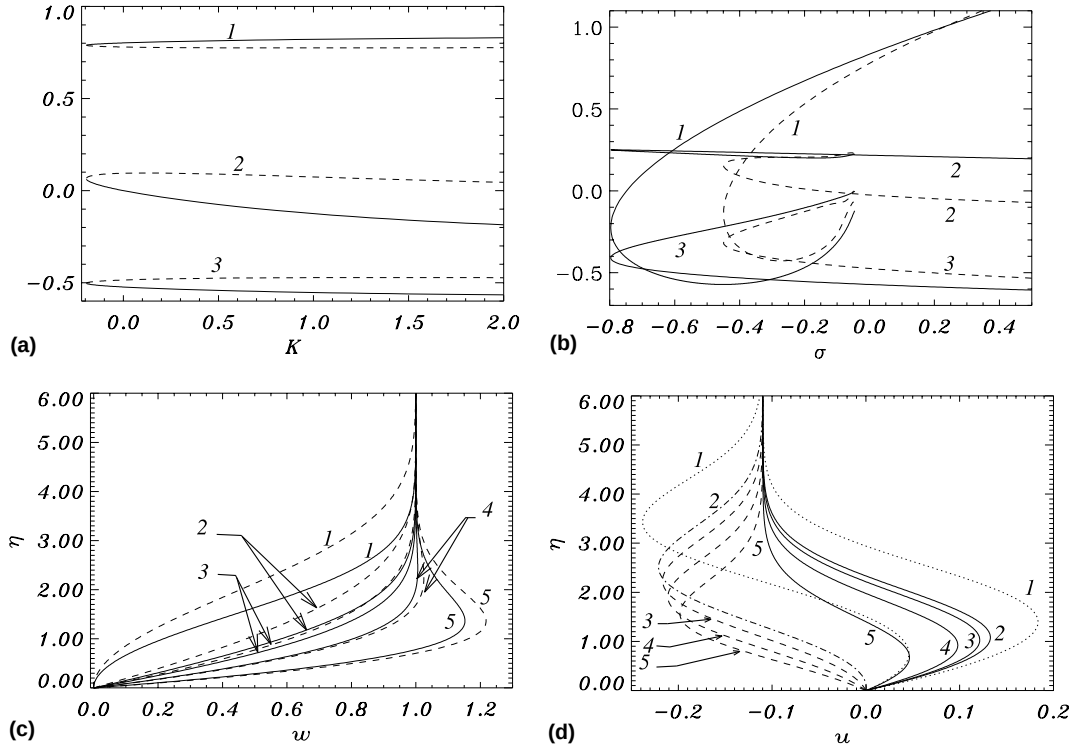

Fig. 6. Corner layer results for a horizontal corner subject to a constant wall heat flux ($\beta = 1/3$) with solid lines corresponding to the upper branch solution and broken lines to the lower branch one. In (a) and (b) curves 1–3 correspond, respectively, to $w'(0)$, $u'(0)$, $\theta'(0)$; in (a) $\sigma = 0.0$ while in (b)–(d) $K = 3$. Curves 2–5 depict results for $\sigma = -0.2, 0.0, 0.5, 2.0$ while curve 1 designate the zero primary flow wall shear stress situations for which $\sigma = -0.435$ for the lower branch solution and -0.748 for the upper branch one.

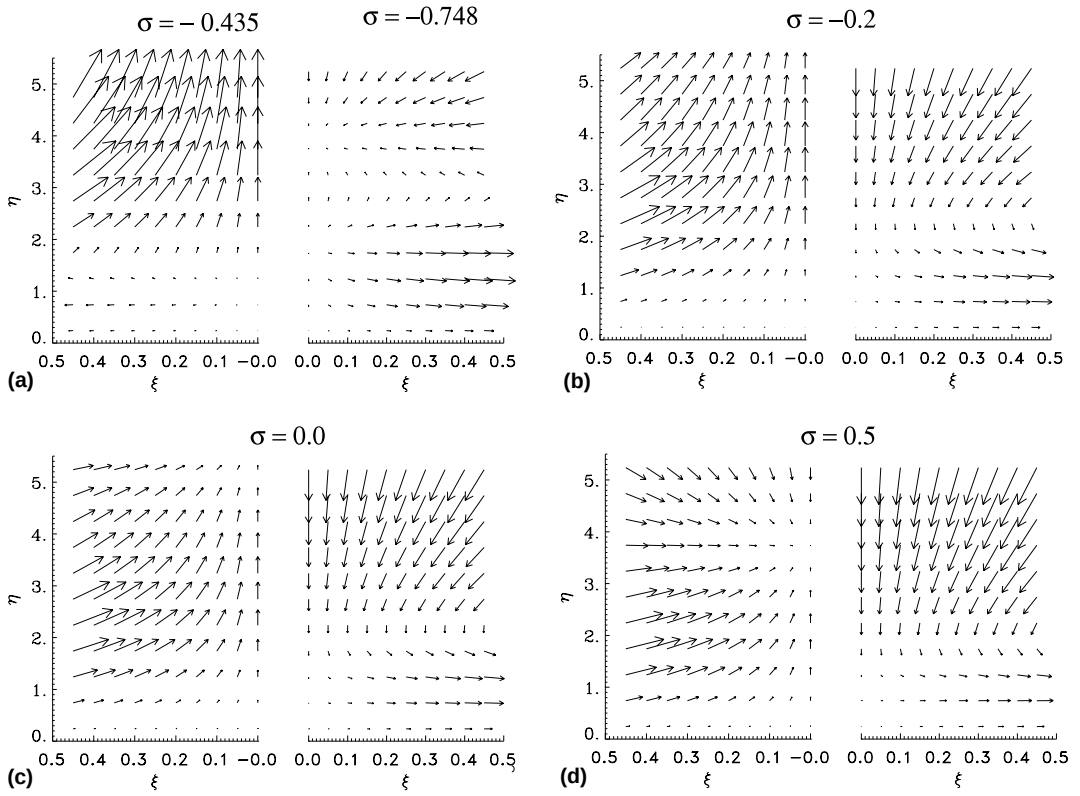

Fig. 7. Corner layer secondary flow vector plots for a horizontal corner (with $K = 3.0$, $\beta = 1/3$): (a) depicts results corresponding to zero primary flow wall shear stress, (a)–(d) the left- and right-hand side plots correspond, respectively, to the lower and upper branch solutions.

4.3. $K \to -\infty$

When $K \to -\infty$ the boundary layer becomes considerably thinner with η becoming $O(\exp(K/\pi)$, see in this connection [19] for the corresponding problem (but without convection, $\sigma = 0$) of three-dimensional point stagnation flow into a corner, or [17] for that of a corner layer flow along a convex corner of arbitrary angle (again with $\sigma = 0$). For the present situation, the solution can be obtained by writing $\eta = (2\mathrm{sgn}(\beta)/\beta)^{1/2} \exp(K/\pi)\zeta$ and

$$\begin{aligned} F_0 &\mapsto \frac{1}{2}\beta\mathrm{sgn}(\beta) \\ &\quad \times \exp(-2K/\pi)F(\zeta) + O(\exp(-K/\pi), \\ G_0 &\mapsto \frac{1}{2}\left(2\beta\mathrm{sgn}(\beta)\right)^{1/2} \\ &\quad \times \exp(-K/\pi)G(\zeta) + O(1), \\ (H_0, \theta_0) &\mapsto (H, \theta) + O\left(\exp(K/\pi)\right) \end{aligned} \tag{4.33}$$

with $\sigma \mapsto \sigma \exp(-3K/\pi)$ in order to retain mixed-convection boundary layer motion.

Inserting these definitions into Eqs. (4.22)–(4.26) yields

$$G''' + GG'' + 1 - G'^2 = 0, \quad F = -G', \tag{4.34}$$

for the motion in the x–y plane. For the streamwise motion and temperature field, we find

$$\begin{aligned} &H'' + GH' + \sigma\left(\frac{2\mathrm{sgn}(\beta)}{\beta}\right)^{3/2}(2-\beta)^{1/2} \\ &\quad \times \left[2\beta\int_{\zeta}^{\infty}\theta(\tau)\,\mathrm{d}\tau + (1-\beta)\zeta\theta\right] = 0, \\ &\frac{1}{Pr}\theta'' + G\theta' = 0, \end{aligned} \tag{4.35}$$

respectively, in which a prime denotes differentiation with respect to ζ. The pertinent boundary conditions in this case are $F = G = G' = H$, $\theta = 1 = 0$ at $\zeta = 0$, and when $\zeta \to \infty$ are $F \to -\mathrm{sgn}(\beta)$, $G' \to \mathrm{sgn}(\beta)$, $H \to 1$, and $\theta \to 0$.

Few observations deserve making here. First, when $\sigma = 0$ we recover the corresponding equations for (F, G, H) found in [17] for streamwise flow in almost planar corners. In this case it can be shown that

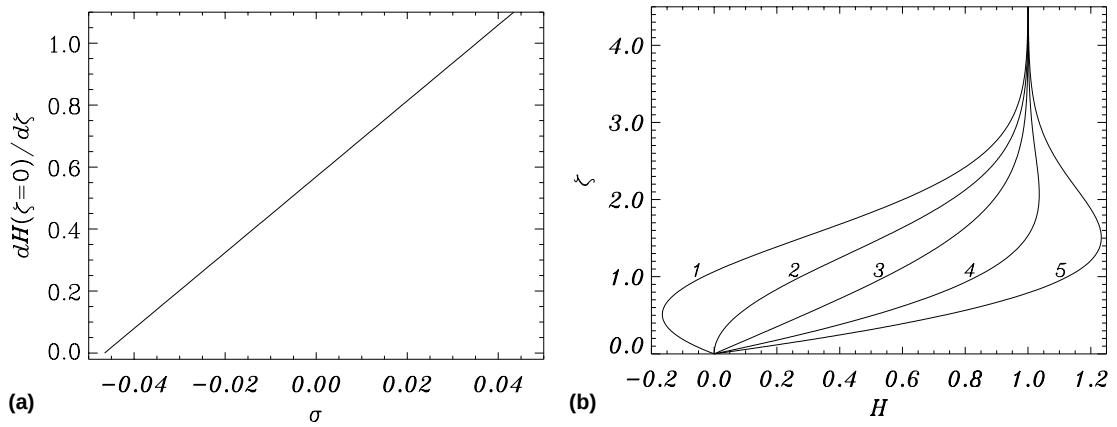

Fig. 8. Primary flow results for the convex corner limit $K \to -\infty$: (a) shows that the wall shear stress $H'(0)$ varies linearly with σ, (b) velocity profiles 1–5 correspond to $\sigma = -0.1, -0.0465, 0.0, 0.05, 1.0$ the second of which pertains to the zero wall shear stress case.

solutions exist only when $\beta > 0$ since G grows exponentially as $\zeta \to \infty$ for $\beta < 0$. Accordingly the G-equation together with the boundary conditions have now the same solution as for a two-dimensional stagnation flow. Second, the above equations suggest that corner boundary layer flow for convex corners is primarily determined by the motion in the x–y plane as observed first in [19] (when $\beta = 1$) and confirmed later in [17] for the general case of a convex corner of arbitrary angle. When $\sigma \neq 0$, this suggests that the motion in the x–y plane is not influenced, to the order considered here, by the thermal field; it is rather the latter which is affected in a forced-convection like manner by the former. On the other hand, the flow in the streamwise direction is determined now by motion in the cross-plane and is subject to combined forced and free convections. At this juncture, it is worth noting that the complete problem leads to similar results, this can easily be checked by only adding mixed-convection to the convex corner problem treated in [17]. The reason for such a behaviour arises simply from having the streamwise equation uncoupled from those in the cross plane as well as from the continuity equation. Third, the temperature equation in (4.35) can be obtained from (4.24) on setting $\beta = 1/3$ for a constant wall temperature. As pointed out in [17], the source of these marked differences in the corner layer behaviour for concave and convex corners lies primarily in the role played by the terms in (x/r_0) and $(r/r_0)^{s-1}$ in Eq. (2.1). Clearly the crossflow is characterized by the former term for concave corners ($s > 2$) and by the latter for convex ones ($s < 2$).

Observe also that the wall shear stress is now considerably greater than for concave corners (see also [17,19]), and for similar reasons the wall heat flux becomes larger. This is clearly indicated by the change required in the buoyancy parameter to maintain mixed convection (*i.e.*, the mapping $\sigma \mapsto \sigma \exp(-3K/\pi)$) which becomes rather small for the newly defined σ.

Numerical results of Eq. (4.35) are presented in Fig. 8 where it is immediately seen that $H'(0)$ varies linearly with σ. This behaviour can be deduced by integrating Eq. (4.35) once with respect to ζ. We find that

$$H'(0) = \sigma \int_{\zeta=0}^{\zeta=\infty} \chi(G, \theta)\, \mathrm{d}\zeta$$

in which χ designates a function of G and θ. In Fig. 8(b) a series of primary flow velocity profiles is presented showing the effect of the buoyancy parameter on the flow. Apart from the comments regarding the secondary role played by the primary flow in convex corners, these profiles represent in general a rather typical effect of combined forced and free convection on the primary motion of a boundary layer flow over a horizontal surface; the separation profile is obtained at some stage for opposing flows while aiding flows are characterized by a profile having an overshooting at some $\sigma > 0$.

The author is grateful to the Spanish Ministry of Education for a sabbatical fellowship during which a major part of this work was carried out. He would also like to express his gratitude to Professor M. Velarde for the kind invitation to the Instituto Pluridisciplinar, Universidad Compultense de Madrid, Spain.

References

[1] S.G. Rubin, Incompressible flow along a corner, J. Fluid Mech. 26 (1966) 169–186.
[2] A. Pal, S.G. Rubin, Asymptotic features of viscous flow along a corner, Q. Appl. Math 29 (1971) 91–108.
[3] S.G. Rubin, B. Grossman, Viscous flow along a corner. Part 2. Numerical solution of corner-layer equations, Q. Appl. Math. 29 (1971) 169–186.

[4] S.S. Desai, K.W. Mangler, Incompressible laminar boundary layer flow along a corner formed by two intersecting planes, R.A.E. Technical Report 74062, 1974.
[5] W.H. Barclay, A.H. Ridha, Flow in streamwise corners of arbitrary angle, AIAA J. 18 (1980) 1413–1420.
[6] S.R. Wilkinson, M. Zamir, Cross-flow and vorticity patterns in the corner boundary layer at different corner angles, Aeronaut. Q. 35 (1984) 309–316.
[7] A. Ridha, Sur la couche limite incompressible laminaire le long d'un dièdre, C. R. Acad. Sci. Paris série II t. 311 (1990) 1123–1128.
[8] A. Ridha, On the dual solutions associated with boundary-layer equations in a corner, J. Eng. Math. 26 (1992) 525–537.
[9] M.R. Dhanak, P.W. Duck, The effects of freestream pressure gradient on corner boundary layer, Proc. R. Soc. London A 453 (1997) 1793–1815.
[10] H. El-Gamal, Laminar flow along a corner with boundary layer suction, Ph.D. Thesis, University of London, 1977.
[11] M. Zamir, Similarity and stability of laminar boundary in a streamwise corner, Proc. R. Soc. London A 377 (1981) 269–288.
[12] A.S. Gupta, Heat transfer in a corner with suction, Mech. Res. Commun. 11 (1984) 55–66.
[13] M.H. Kim, M.-U. Kim, D.H. Choi, Forced convective heat transfer in the flow along a corner of arbitrary angle, Mech. Res.Commun. 15 (1988) 274–296.
[14] A. Ridha, Laminar mixed convection in a corner with suction, Mech. Res. Commun. 17 (5) (1990) 327–335.
[15] A. Ridha, On laminar natural convection in a vertical corner, C. R. Acad. Sci. Paris Série IIb t. 328 (2000) 485–490.
[16] A. Ridha, L'écoulement potentiel tridimensionnel le long d'un coin revisité, C. R. Acad. Sci. Paris série IIb t. 321 (1995) 481–487.
[17] A. Ridha, Flow along streamwise corners revisited, J. Fluid Mech. (2001), submitted.
[18] F.K. Moore, Three-dimensional boundary layer theory, Adv. Appl. Mech. 4 (1956) 159–228.
[19] F.T. Smith, Three-dimensional stagnation point flow into a corner, Proc. R. Soc. London A 334 (1975) 489–507.
[20] A. Ridha, Aiding flows non-unique similarity solutions of mixed convection boundary layer equations, ZAMP 47 (1996) 341–352.
[21] K. Stewartson, On the free convection from a horizontal plate, ZAMP 9a (1958) 276–281.
[22] A. Ridha, Three-dimensional mixed convection laminar boundary-layer over a horizontal surface in the neighbourhood of a plane of symmetry, Int. J. Heat Mass Transfer 40 (2) (1997) 421–433.
[23] V.V. Sychev, A.I. Ruban, V.V. Sychev, G.L. Korolev, Asymptotic Theory of Separated Flows, Cambridge University Press, Cambridge, 1998.